

Magnetic Field Scaling in Spin Glasses and the Mean-Field Theory

V. S. Zotev and R. Orbach

Department of Physics, University of California, Riverside, California 92521

(Dated: Submitted to PRB on January 14, 2002)

The scaling of the magnetic field dependence of the remanent magnetization for different temperatures and different spin-glass samples is studied. Particular attention is paid to the effect of the de Almeida-Thouless (AT) critical line on spin-glass dynamics. It is shown that results of the mean-field theory of aging phenomena, with two additional experimentally justified assumptions, predict $H/H_{AT}(T)$ scaling for remanent magnetization curves. Experiments on a single crystal Cu:Mn 1.5 at % sample in the temperature interval from $0.7T_g$ to $0.85T_g$ give results consistent with this scaling. Magnetization vs. field curves for different Cu:Mn and thiospinel samples also scale together. These experimental results support the predictions of the mean-field theory of aging phenomena.

PACS numbers: 75.50.Lk, 75.40.Gb

I. INTRODUCTION

Effect of a magnetic field on the spin-glass state is one of the most important open problems in spin-glass physics. Two major theoretical descriptions of spin-glass phenomena have evolved over the past twenty years. One of them is the mean-field theory for the static and dynamical properties of spin glasses, based on the Parisi replica-symmetry-breaking formalism and related ideas.^{1,2} The alternative approach is the droplet model, based on the Migdal-Kadanoff approximation.^{3,4} The two pictures provide very different physical interpretations of observable spin-glass phenomena. This difference is particularly pronounced when spin-glass properties in a magnetic field are considered. The mean-field theory predicts a spin-glass state with replica-symmetry breaking at finite magnetic fields below a critical line in the (T, H) plane.⁵ The droplet model states that a true phase transition occurs at zero magnetic field only. Compelling experimental support for either model has not yet been presented. A detailed analysis of magnetic field effects on real spin glasses can provide information about the comparative validity of the theoretical predictions.

Recent experimental results favor the mean-field picture. Torque measurements have shown that Heisenberg spin glasses with random anisotropy are characterized by a true spin-glass ordered phase at high magnetic fields.⁶ Experimental studies of violations of the fluctuation-dissipation theorem under an increasing field change also support predictions of the mean-field theory.⁷

The remanent magnetization, measured after a change in magnetic field, contains all essential information about spin-glass dynamics. The general features of its field dependence have been studied for various spin glasses.⁸ All experimental results to date, however, have been treated phenomenologically. A comprehensive theoretical picture which can explain these results, and predict the field dependence of measurable quantities over a wide range of field variations, remains lacking. The mean-field theory of aging phenomena,^{2,9,10,11} developed in recent years,

now appears able to provide such a description within the linear response regime. The theory relates the macroscopic relaxation properties of the spin-glass state to microscopic correlations. Many conclusions, derived from this theoretical picture, can be tested experimentally. In the present paper, we study the scaling of magnetization curves with magnetic field for several spin-glass samples. We show that, under some additional experimentally justified assumptions, our experimental results support predictions of this theory.

This paper is organized as follows. In the next Section, the theoretical picture underlying our analysis is outlined. Sec. III.A presents experimental results on the field scaling for different temperatures. In Sec. III.B, experimental data for different samples are compared. Section IV summarizes our conclusions.

II. THEORETICAL BACKGROUND AND SCALING PREDICTIONS

The *equilibrium* susceptibility of an Ising spin glass, identified with the equilibrium value of the experimental field-cooled susceptibility, is given by the following expression:¹²

$$\chi_{FC} = [1 - \int_0^1 q(x)dx]/T . \quad (1)$$

This susceptibility includes contributions from different pure equilibrium states with the nontrivial distribution of overlaps $q(x)$. The value $q(1) = q_{EA}$ is the equilibrium Edwards-Anderson order parameter, and $q(0) = q_{min}$ is the minimum possible overlap, nonzero in the presence of a magnetic field. The spin-glass state is chaotic in magnetic field,¹² meaning that the average equilibrium overlap of two states at slightly different values of magnetic field is equal to q_{min} .

The *linear response* susceptibility, identified with the experimental zero-field-cooled susceptibility at short ob-

ervation times $\tau = t - t_w$, is given by the fluctuation-dissipation theorem (FDT) in its integral form:¹¹

$$\chi(t, t_w) = [1 - C(t, t_w)]/T . \quad (2)$$

Here, $C(t, t_w)$ is the autocorrelation function for a system of N Ising spins, defined as follows:

$$C(t, t_w) = (1/N) \sum_{i=1}^N \langle S_i(t) S_i(t_w) \rangle . \quad (3)$$

The linear response susceptibility is associated with transitions within a single pure state. The difference between the values of the field-cooled and zero-field-cooled susceptibilities is a manifestation of replica-symmetry breaking.¹²

Spin-glass dynamics is limited to a single ergodic component, because the energy barriers, separating the pure equilibrium states, are divergent in the thermodynamic limit. The long-time dynamics within one pure state can be viewed as a series of transitions from a trap to a deeper trap.² The barriers surrounding these traps are high, but finite, and “traps encountered at long times tend to increasingly resemble the actual states contributing to the equilibrium”.¹³ This interpretation leads to a description of asymptotic spin-glass dynamics, algebraically similar to the static replica-symmetry-breaking formalism.

Dynamical definitions of q_{EA} and q_{min} are given in terms of the correlation function:^{2,11}

$$q_{EA} = \lim_{\tau \rightarrow \infty} \lim_{t_w \rightarrow \infty} C(t_w + \tau, t_w) ; \quad (4)$$

$$q_{min} = \lim_{\tau \rightarrow \infty} C(t_w + \tau, t_w) . \quad (5)$$

Eq. (5) means that, after a small field change following a finite waiting time t_w , the system evolves towards an equilibrium state that has the minimum possible correlation with the initial state at $t = t_w$.

Experiments¹⁵ and computer simulations¹⁶ suggest the following picture of spin-glass relaxation. At short observation times, $\tau \ll t_w$, the relaxation is fast (on the linear time scale) and equilibrium in nature. The correlation function, Eq. (3), drops from 1 to q_{EA} . The fluctuation-dissipation theorem holds, and the susceptibility is given by Eq. (2). At longer observation times, $\tau > t_w$, the relaxation is very slow and t_w -dependent. The correlation decreases from q_{EA} to q_{min} . The FDT is violated, and the zero-field-cooled susceptibility relaxes towards the equilibrium value, presumably given by Eq. (1).

It is proposed in the mean-field theory of aging phenomena² that, for large t_w , the susceptibility depends on its time arguments only through the correlation function, i.e. $\chi = \chi[C(t, t_w)]$, even when the fluctuation-dissipation theorem is violated. The susceptibility $\chi(C)$ is a piecewise function.^{10,11} It is linear in the equilibrium regime:

$$\chi(C) = [1 - C]/T , \quad q_{EA} \leq C < 1 . \quad (6)$$

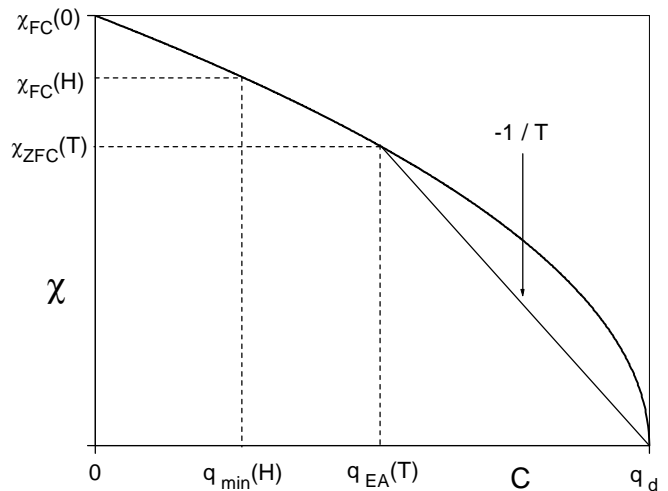


FIG. 1: A diagram of the spin-glass relaxation at temperature T after magnetic field H is applied. The thick line is the master curve $\tilde{\chi}(C)$. The straight line segment from $(q_d, 0)$ to (q_{EA}, χ_{ZFC}) represents the equilibrium relaxation regime. The slope is $-1/T$. The master curve segment from (q_{EA}, χ_{ZFC}) to (q_{min}, χ_{FC}) corresponds to the aging regime.

In the aging regime, the relaxing part of the susceptibility, $\chi_{ag}(C)$, is nonlinear:

$$\chi(C) = [1 - q_{EA}]/T + \chi_{ag}(C) , \quad q_{min} < C < q_{EA} . \quad (7)$$

The well-known Parisi-Toulouse approximation¹⁴ makes use of the following assumptions: the equilibrium susceptibility, Eq. (1), is independent of temperature, while q_{EA} and q_{min} are functions of only temperature and magnetic field, respectively. The dynamical version of this approximation implies^{10,11} that the function $\chi_{ag}(C)$ in Eq. (7) is both T - and H -independent. This means that the dependence $\chi(C)$ is universal in the aging regime, and follows a master curve $\tilde{\chi}(C)$. If the value of the susceptibility at the limit of validity of the FDT, i.e. at $C = q_{EA}$, is denoted as χ_{ZFC} , one can write the following:

$$\chi_{FC} = \chi_{FC}(H) ; \quad \chi_{ZFC} = \chi_{ZFC}(T) . \quad (8)$$

Fig. 1, taken directly from Cugliandolo *et al.*,¹¹ displays the master curve $\tilde{\chi}(C)$. Each point on this curve corresponds to a transition from the equilibrium to the aging regime at some temperature $0 < T < T_g$. The quantity q_d is the initial correlation $C(t_w, t_w)$, which depends on the number of spin components. It appears instead of unity in Eqs. (6) and (7) if the spins are not Ising.

The contribution of this paper is the experimental study of the magnetic field dependence of the remanent susceptibility $\chi_{FC}(H) - \chi_{ZFC}(T)$. According to Fig. 1, it is related to the difference $q_{EA}(T) - q_{min}(H)$. In order to derive a magnetic field scaling relationship, we must introduce two additional assumptions. First, we consider relatively high temperatures and assume that the master curve $\tilde{\chi}(C)$ at low C can be approximated by a straight

line. Then the triangles in Fig. 1 are geometrically similar for all allowed T and H , and the following relation holds:

$$\frac{\chi_{FC}(H) - \chi_{ZFC}(T)}{\chi_{FC}(0) - \chi_{ZFC}(T)} = \frac{q_{EA}(T) - q_{min}(H)}{q_{EA}(T)}. \quad (9)$$

Second, let us suppose that $q_{min}(H)$ is a homogeneous function of order p , that is $q_{min}(aH) = a^p q_{min}(H)$ with some $p \neq 0$. Then, introducing the critical AT field, one can write:

$$\frac{q_{min}(H)}{q_{EA}(T)} = \frac{q_{min}(H)}{q_{min}[H_{AT}(T)]} = \frac{q_{min}[H/H_{AT}(T)]}{q_{min}(1)}. \quad (10)$$

Here we used the condition¹² that the de Almeida-Thouless critical line is defined by $q_{min} = q_{EA}$. It follows from Eqs. (9) and (10) that the remanent susceptibility, $\chi_{FC}(H) - \chi_{ZFC}(T)$, should scale as H/H_{AT} . This is a consequence of the proposed universality of $\tilde{\chi}(C)$. The present paper is devoted to the experimental study of this field scaling. We shall also use our experimental data to justify the two assumptions which lead to Eqs. (9) and (10).

III. EXPERIMENTAL RESULTS AND ANALYSIS

Before presenting our experimental results, we would like to make some preliminary remarks.

Predictions of the mean-field theory of aging phenomena, mentioned in the previous section, are expected to hold only in the linear response regime. This means that a change in magnetic field, acting as a probe of the spin-glass state, must be much smaller than the AT field at a given measurement temperature. A larger field change would lead to a deviation from linear response. The measured zero-field-cooled susceptibility would then become field-dependent, and the arguments, based on Fig. 1, could not be used.

Eqs.(8)-(10) can be applied to experimental data only if the zero-field-cooled susceptibility is measured at the end of the fluctuation-dissipation regime. For relatively short waiting times, the transition from one regime to the other is not well defined. Computer simulations show¹⁶ that violation of the FDT becomes visible at observation times τ at least one order of magnitude shorter than the waiting time t_w , the violation becoming strong at $\tau \approx t_w$. All of our experiments have been performed on a commercial Quantum Design SQUID magnetometer. The shortest possible observation time is about 40 s. The typical effective cooling time is 600 s because of the rather low cooling rate near the measurement temperature. By the time the first experimental point is taken, the fast initial decay is essentially over. Thus, the short-time measurements yield results, which are approximately at the end of the fluctuation-dissipation regime, even at zero waiting time.

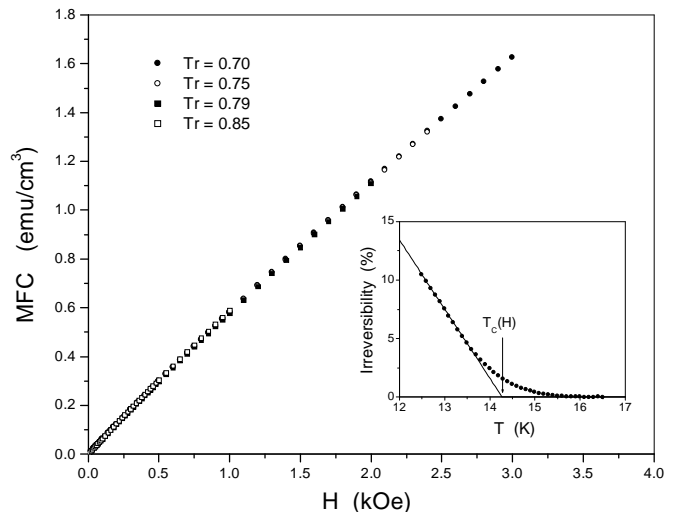


FIG. 2: The field-cooled magnetization of the single crystal Cu:Mn 1.5 at % for different temperatures $Tr = T/T_g$. The inset displays the irreversibility $(1 - ZFC/MFC) * 100\%$ as a function of temperature for $H = 200$ Oe.

In our analysis, we use experimental values of magnetizations instead of susceptibilities. This is because numerical differentiation requires fitting, and any fitting involves interpretation. Of course, all arguments regarding the field scaling apply to magnetizations as well. For example, Eqs. (9) and (10) suggest that the slope of the remanent magnetization, $MFC - ZFC$, at field H , divided by its slope at $H = 0$, will be a function of $H/H_{AT}(T)$. The rest of this Section presents our experimental results, which will support this prediction.

A. Field scaling for different temperatures

In order to test validity of Eqs. (9) and (10), we measured the field-cooled (MFC) and zero-field-cooled (ZFC) magnetizations as functions of the field $H = \Delta H$ for four different temperatures. All results reported in this subsection were obtained for a single crystal Cu:Mn 1.5 at %. It is a long-range Heisenberg spin glass with a glass temperature T_g of approximately 15.2 K. The experimental phase diagram for this sample will be presented elsewhere. The measurements of the ZFC magnetization were made at the shortest observation time, with zero waiting time between the cooling and application of the field.

Fig. 2 exhibits the field dependence of the field-cooled magnetization. The data are presented as taken, without any rescaling of the field or adjustment of the magnetization magnitude. Error bars are considerably smaller than the symbol sizes and are not shown in the figure. The same applies to the other figures in this paper that do not exhibit error bars. It is evident that $MFC(H)$ is virtually independent of temperature. Therefore, the Parisi-Toulouse approximation works rather well in the

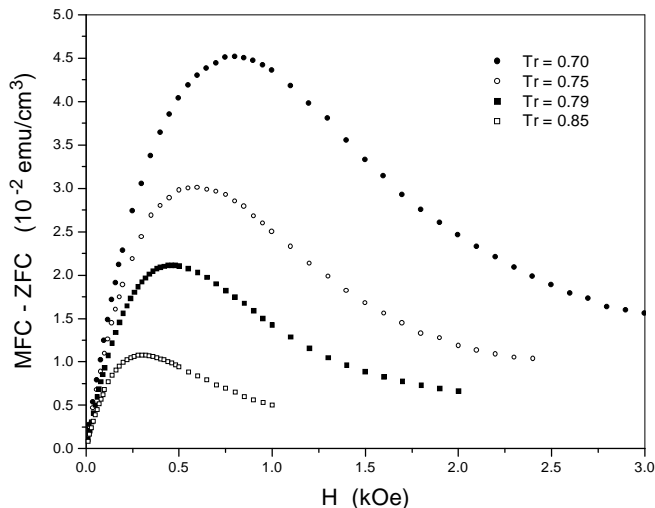


FIG. 3: The remanent magnetization of the single crystal Cu:Mn 1.5 at % as a function of field for the same temperatures as in Fig. 2.

case of this sample. This appears to be a common feature of Cu:Mn spin glasses.¹¹

The spin-glass phase is characterized by the difference between the field-cooled and zero-field-cooled magnetizations. The inset of Fig. 2 displays temperature dependence of the $MFC - ZFC$ irreversibility at fixed magnetic field. Weak irreversibility in the Cu:Mn 1.5 at % single crystal appears slightly above the glass temperature of 15.2 K. The irreversibility becomes strong as temperature is lowered, evolving to a region where it increases linearly with a large slope. The strong $MFC - ZFC$ irreversibility is interpreted as a sign of the spin-glass phase transition. The T -intercept of the linear fit in this region is taken as the crossover temperature $T_c(H)$. These crossover temperatures, determined for different magnetic fields H , define the AT line.

Fig. 3 displays field dependences of the $MFC - ZFC$ irreversibility for different temperatures. The four curves are similar in shape, but the field scale for each depends on the measurement temperature. The peak in $MFC - ZFC$ corresponds to a strong violation of linear response. It turns out that the position of this peak depends on the value of the AT field.

The experimental AT line for the Cu:Mn 1.5 at % single crystal sample is exhibited in Fig. 4. One can see that this line has the functional form $T_g - T_c(H) \propto H^{2/3}$, typical of the AT line⁵ in the Sherrington-Kirkpatrick (SK) model.¹⁷ Fig. 4 also shows temperature dependence of the position of the peak in $TRM(H)$, which we denote as $H_M(T)$, and of the peak in $(MFC - ZFC)(H)$, which we refer to as $H_m(T)$. The thermoremanent magnetization, TRM , is not equal to $MFC - ZFC$ if linear response is violated, and $H_m < H_M$ for any temperature. However, both $H_M(T)$ and $H_m(T)$ are proportional to the critical field $H_{AT}(T)$, according to Fig. 4. The peak in $(MFC - ZFC)(H)$ is easier to identify than

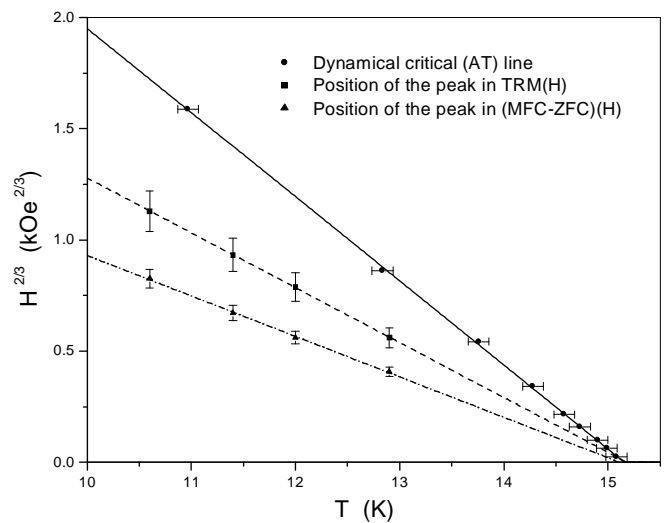


FIG. 4: From top to bottom: $H_{AT}(T)$, the experimental AT critical line; $H_M(T)$, the position of the peak in $TRM(H)$; $H_m(T)$, the position of the peak in $(MFC - ZFC)(H)$.

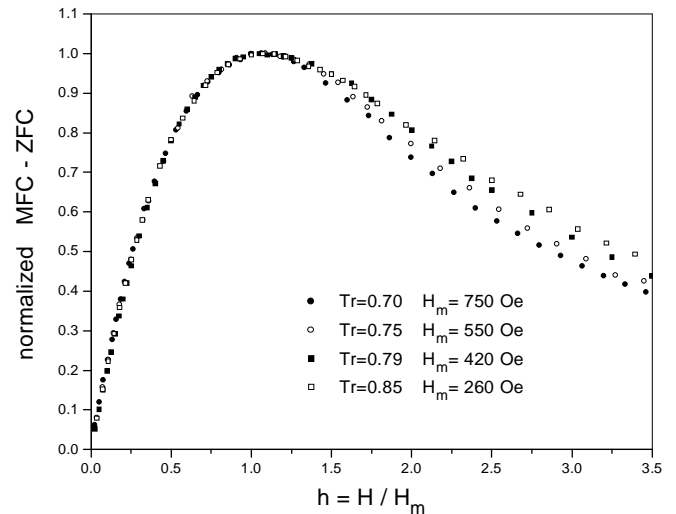


FIG. 5: Scaling of the remanent magnetization curves for different temperatures. The positions of the peaks, $H_m(T)$, are used as scaling parameters.

the AT line itself. In this subsection, we shall use its position, $H_m(T)$, as the field scaling parameter, and consider H/H_m scaling instead of H/H_{AT} scaling.

Fig. 5 exhibits the $MFC - ZFC$ irreversibility, normalized by its value at H_m , and plotted versus $h = H/H_m$. One can see that the curves for different temperatures fall on top of one another for $h < 1$. This is the interval of field variations where linear response holds, at least approximately. Therefore, the field scaling, predicted by Eqs. (9) and (10), is indeed observed in spin-glass experiments. For $h > 1$, however, the scaling is rather poor. There is strong nonlinearity in the spin-glass response in this regime, and the mean-field theory of aging phenomena will not be applicable.

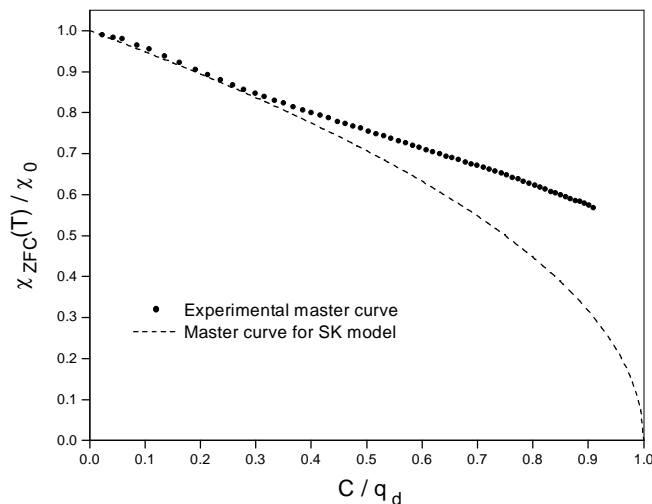


FIG. 6: The master curve $\tilde{\chi}(C)$ for the single crystal Cu:Mn 1.5 %, estimated from the experimental $\chi_{ZFC}(T)$ dependence. The master curve for the SK model is $\tilde{\chi} = (1 - C)^{1/2}$.

Of course, nonlinearity by itself does not necessitate lack of scaling. There are at least two probable reasons for the observed differences in high-field behavior at different temperatures. First, freezing of the transverse spin components¹⁸ in Heisenberg spin glasses produces the weak irreversibility in the longitudinal direction. Second, the distribution of glass temperatures, always present in real samples, has a stronger effect at higher measurement temperatures and higher fields. The inset of Fig 2 shows that there is a significant remanence at the crossover temperature. It corresponds to the remanence near the AT line at $h \approx 3.5$ in Fig. 5. Obviously, we cannot expect the H/H_{AT} scaling to hold precisely in this region.

The scaling of the $MFC - ZFC$ curves in Fig. 5 suggests, *a posteriori*, that the assumptions leading to Eqs. (9) and (10) are in fact reasonable. In order to clarify this conclusion, we determined the master curve $\tilde{\chi}(C)$ according to the method of Cugliandolo *et al.*¹¹ If the zero-field cooled susceptibility is measured at the limit of validity of the FDT, the corresponding correlation can be obtained from Eq. (6). Then the values of $\chi_{ZFC}(T)$ for different temperatures, plotted vs. $C(T)$, span the master curve $\tilde{\chi}(C)$. The experimental master curve is shown in Fig. 6. The data points were taken in the interval from $T = 2.4$ K to $T = 15.0$ K at the same low field $H = 16$ Oe. Each measurement was independent of the others, and included a quench from above the glass temperature.

Fig. 6 demonstrates that the experimental dependence of χ on C is close to linear over a wide range of correlations. This justifies the assumption underlying Eq. (9): the master curve $\tilde{\chi}(C)$ at relatively low C can be approximated by a straight line.

The experimental data for the AT critical line in Fig. 4 suggest that, to the leading order of magnitude, $q_{min}(H) \propto H^{2/3}$. Therefore, $q_{min}(H)$ is indeed a homo-

geneous function of order $p = 2/3$, and the assumption underlying Eq. (10) is also verified.

These arguments, of course, should be taken with caution. A reliable experimental determination of the master curve $\tilde{\chi}(C)$ would require independent measurements of both the susceptibility and the correlation. Fig. 6 only gives an idea of how the real curve may look. In particular, the experimental master curve in Fig. 6 does not exhibit a significant downturn at high values of C/q_d . The difference between this curve and the theoretical curve $\tilde{\chi} = (1 - C)^{1/2}$ for the SK model¹⁰ is very pronounced in that region. This problem, however, is beyond the scope of the present paper. It is also evident that we cannot expect the above two assumptions to hold beyond the leading order of magnitude even at high enough temperatures and low values of C . It would be correct to say, therefore, that the AT field defines a characteristic field scale at any temperature, but the scaling itself is always approximate.

B. Field scaling for different samples

The results of the previous subsection suggest that the master curve $\tilde{\chi}(C)$ in Fig. 1 is universal, that is T and H independent, thus supporting the Parisi-Toulouse approximation. It would be interesting to see, therefore, if this curve depends on the choice of sample. Different spin-glass samples have different microscopic properties, and, consequently, different effective magnetic field scales. If the Parisi-Toulouse approximation holds, the magnetic field H appears in the analysis through $q_{min}(H)$ only. Therefore, if the master curve $\tilde{\chi}(C)$ is sample independent, and $q_{min}(H)$ has always the same functional form, we can expect the scaling of magnetization curves to hold for different samples.

In order to study this issue, we measured the field-cooled (MFC) and the thermoremanent (TRM) magnetizations as functions of $H = \Delta H$ for five different spin-glass samples. In addition to the single crystal Cu:Mn 1.5 at %, described previously, we used a single crystal Cu:Mn 0.6 at %, with the glass temperature of about 6.0 K. Both samples have been prepared in Kammerlingh Onnes Laboratory (Leiden). Similar single crystals have been used for neutron-scattering experiments.¹⁹ The other three of our samples are polycrystalline. The polycrystal Cu:Mn 6.0 at % has been extensively studied before.²⁰ Its glass temperature is near 31.0 K. The thiospinel $CdCr_{1.7}In_{0.3}S_4$ is an insulating short-range spin glass with $T_g = 16.7$ K. It has also been studied in detail.²¹ The second thiospinel sample, used in our analysis, has been obtained from the part of the first sample by sifting it through a 100 nm mesh. This was done to probe the finite-size effects.²² The sifted thiospinel has a slightly lower glass temperature $T_g \approx 16.5$ K.

Fig. 7 displays the thermoremanent magnetizations versus the field H for these five samples. All data points are taken at the same short observation time of 90 s after

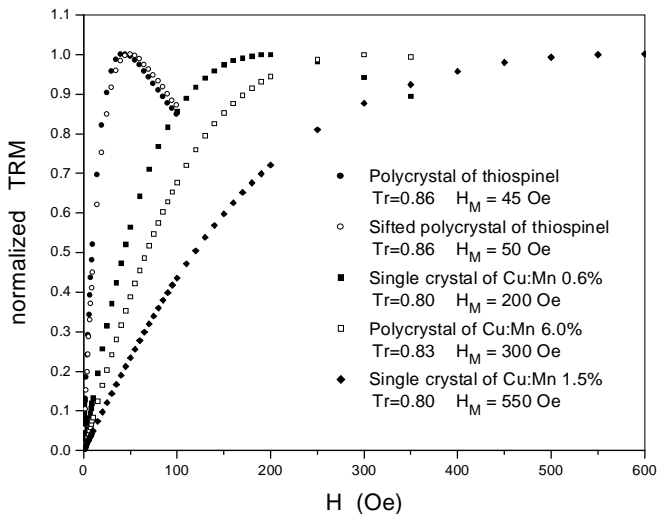


FIG. 7: Thermoremanent magnetization for five spin-glass samples measured at $t_w = 30 \text{ min}$. The positions of the maxima, $H_M(T)$, are proportional to the AT fields.

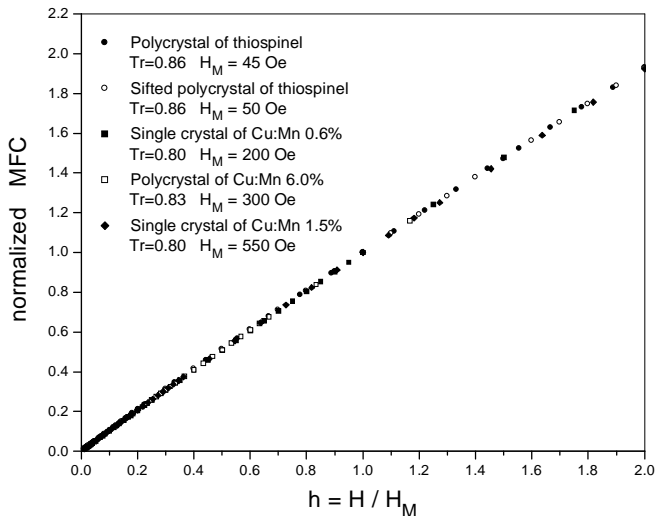


FIG. 8: Scaling of the field-cooled magnetization curves for the five samples. The values of $H_M(T)$ are used as scaling parameters.

the field is cut to zero. The waiting time between the end of the cooling process and the field change is 30 min . The reduced measurement temperatures, $Tr = T/T_g$, for different samples are not exactly the same, but it is not very important considering the results of Sec. III.A. It is evident from Fig. 7 that different samples have very different characteristic field scales. The effect of the same magnetic field is strongest in the case of the thiospinel, and it is much less pronounced for the single crystal Cu:Mn 1.5 at %. The characteristic field scales for these two samples differ by one order of magnitude.

One can see from Fig. 7 that each $TRM(H)$ curve has a maximum. According to Fig. 4, the position of this maximum, $H_M(T)$, is proportional to the corresponding

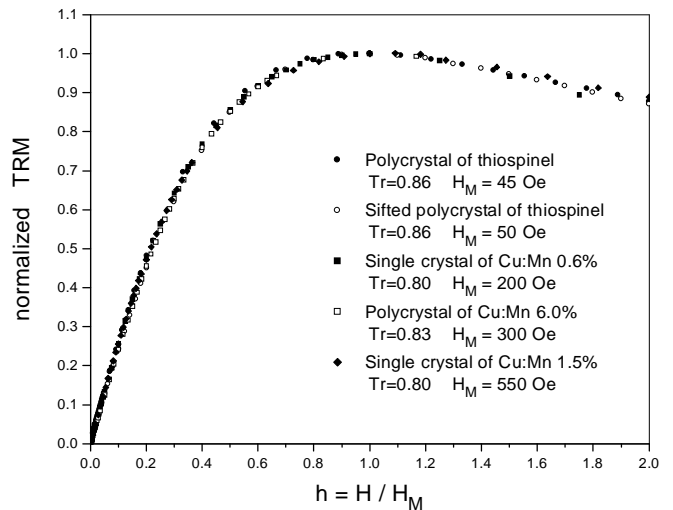


FIG. 9: Scaling of the thermoremanent magnetization curves from Fig. 7, plotted vs. H/H_M .

AT field, $H_{AT}(T)$. In this subsection, we will characterize each sample by its value of H_M , and consider H/H_M scaling instead of the H/H_{AT} scaling.

Fig. 8 exhibits experimental $MFC(H)$ curves, plotted versus $h = H/H_M$ and normalized by their values at $h = 1$. All five curves seem to scale well together. This suggests that, apart from the differences in the field scales, the physical mechanism behind the observed field dependence is the same for all these very different samples. Fig. 8 suggests that the functional form of $q_{min}(H)$ is essentially independent of sample.

The experimental $TRM(H)$ curves from Fig. 7, plotted versus the reduced field $h = H/H_M$, are presented in Fig. 9. The overall scaling is surprisingly good, taking into account the diversity in properties of the five samples. We conclude that the observed nonlinearity in spin-glass response has the same physical origin for all samples.

The major deviations from perfect scaling seem to result from finite-size effects. They are not clearly visible in Fig. 9, but can be seen in Fig. 10. This figure exhibits the normalized TRM curves, divided by $h = H/H_M$, for the two thiospinel samples. The full thiospinel sample with $T_g \approx 16.7 \text{ K}$ has a broad distribution of particle sizes. The sifted thiospinel sample with $T_g \approx 16.5 \text{ K}$ consists of particles smaller than 100 nm in diameter. The measurement temperatures were 14.4 K and 14.2 K , respectively, so that the reduced temperature $Tr = T/T_g$ has the same value of 0.86 for both samples.

Two conclusions can be derived from the data in Fig. 10. First, the characteristic field for the sifted sample is about 10% higher than for the full sample. This is consistent with the mean-field-theory predictions. The differences in free energies per site for different equilibrium states are of the order of $1/N$, where N is the total number of spins. For smaller N , a stronger perturbation is needed to redistribute these energy differences and thus

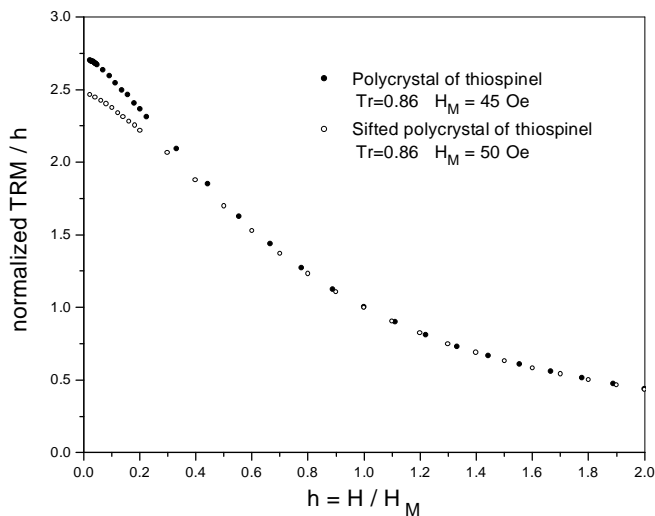


FIG. 10: Comparison of results for the two thiospinel samples. The differences in the values of H_M and in the low-field behavior can be attributed to the finite-size effects on the spin-glass properties of the sifted sample.

reshuffle the weights of different pure states.²³ Therefore, nonlinearity in response appears at higher field changes for smaller particles. The second conclusion is that the differences in behavior between the full sample and the sifted sample are more pronounced in the low-field region. This is also in agreement with results of the mean-field theory. The magnetic correlation length, ξ_H , drops sharply as the change in field increases.²³ If the field change makes two spins uncorrelated, existence of a grain wall between them becomes irrelevant. Thus, finite-size effects on spin-glass dynamics are more pronounced at lower field changes. Of course, there may be other reasons for the differences between the two thiospinel samples.

Apart from the finite-size effects, the overall scaling in Fig. 9 is impressive, and demonstrates the validity of

the theoretical analysis in Section II. Our results suggest that both the master curve $\tilde{\chi}(C)$ and the function $q_{min}(H/H_{AT})$ are essentially independent of the nature of a particular spin-glass sample. This is a strong evidence in support of mean-field theory.

IV. CONCLUSION

The mean-field theory of aging phenomena establishes a relation between the susceptibility χ and the correlation C in both the equilibrium and aging regimes of spin-glass relaxation. It suggests that $\chi(C)$ is a universal function in the aging regime, and that the remanent susceptibility $\chi_{FC} - \chi_{ZFC}$ is related to the difference $q_{EA} - q_{min}$ in the values of the correlation. We have shown in this paper that two additional assumptions, the linearity of $\chi(C)$ in the aging regime and the homogeneity of $q_{min}(H)$ in a wide range of fields, lead to a prediction of $H/H_{AT}(T)$ scaling of the remanent susceptibility curves. Our experiments on the single crystal Cu:Mn 1.5 at % demonstrate the existence of such scaling in the temperature interval $T/T_g = 0.7...0.85$. Moreover, the thermoremanent magnetization curves for different spin-glass samples also scale quite well together if plotted vs. H/H_{AT} . These results indicate that there is universality for the magnetic properties of different spin glass systems at different temperatures. They also suggest that the magnetic field effects on spin-glass dynamics in the linear response regime are correctly described by the mean-field theory of aging phenomena.

We appreciate the courtesy of Professor J. A. Mydosh from Kammerlingh Onnes Laboratory (The Netherlands) who kindly provided us with the Cu:Mn single crystal samples. We are also eternally grateful to Dr. J. Hammann and Dr. E. Vincent from CEA Saclay (France) for giving us one half of their thiospinel sample. We thank Dr. G. G. Kenning for his constant interest and support.

¹ M. Mezard, G. Parisi, and M. A. Virasoro, *Spin Glass Theory and Beyond* (World Scientific, Singapore, 1987).

² J.-P. Bouchaud, L. F. Cugliandolo, J. Kurchan, and M. Mezard in *Spin Glasses and random fields* ed. by A. P. Young (World Scientific, Singapore, 1997).

³ D. S. Fisher and D. A. Huse, *Phys. Rev. Lett.* **56**, 1601 (1986); *Phys. Rev. B* **38**, 373 (1988); **38**, 386 (1988).

⁴ A. A. Migdal, *Sov. Phys. JETP* **42**, 743 (1975); L. P. Kadanoff, *Ann. Phys.* **91**, 226 (1975).

⁵ J. R. L. de Almeida and D. J. Thouless, *J. Phys. A* **11**, 983 (1978).

⁶ D. Petit, L. Fruchter, and I. A. Campbell, *Phys. Rev. Lett.* **83**, 5130 (1999); cond-mat/0111129.

⁷ V. S. Zotev and R. Orbach, submitted, cond-mat/0112489.

⁸ J. L. Tholence and R. Tournier, *J. Phys. Colloque (France)* **4**, 229 (1974); H. Bouchiat and P. Monod, *J. Mag. Magn.*

Mat. **30**, 175 (1982); P. Nordblad, L. Lundgren and L. Sandlund, *Europhys. Lett.* **3**, 235 (1987).

⁹ S. Franz, M. Mezard, G. Parisi, and L. Peliti, *Phys. Rev. Lett.* **81**, 1758 (1998); *J. Stat. Phys.* **97**, 459 (1999).

¹⁰ E. Marinari, G. Parisi, F. Ricci-Tersenghi, and J. J. Ruiz-Lorenzo, *J. Phys. A* **31**, 2611 (1998).

¹¹ L. F. Cugliandolo, D. R. Grempel, J. Kurchan, and E. Vincent, *Europhys. Lett.* **48**, 699 (1999).

¹² G. Parisi, *Phys. Rev. Lett.* **50**, 1946 (1983); *Physica A* **124**, 523 (1984).

¹³ L. F. Cugliandolo and J. Kurchan, *J. Phys. A* **27**, 5749 (1994).

¹⁴ G. Parisi and G. Toulouse, *J. Phys. Lett. (France)* **41**, L361 (1980); J. Vannimenus, G. Toulouse and G. Parisi, *J. Phys. (France)* **42**, 565 (1981).

¹⁵ M. Ocio, H. Bouchiat, and P. Monod, *J. Phys. Lett.*

- (France) **46**, L647 (1985); L. Lundgren, P. Nordblad, P. Svedlindh, and O. Beckman, *J. Appl. Phys.* **57**, 3371 (1985).
- ¹⁶ J. O. Andersson, J. Mattsson, and P. Svedlindh, *Phys. Rev. B* **46**, 8297 (1992); S. Franz and H. Rieger, *J. Stat. Phys.* **79**, 749 (1995).
- ¹⁷ D. Sherrington and S. Kirkpatrick, *Phys. Rev. Lett.* **35**, 1792 (1975).
- ¹⁸ M. Gabay and G. Toulouse, *Phys. Rev. Lett.* **47**, 201 (1981); D. M. Cragg, D. Sherrington, and M. Gabay, *Phys. Rev. Lett.* **49**, 158 (1982).
- ¹⁹ F. J. Lamelas, S. A. Werner, S. M. Shapiro, and J. A. Mydosh, *Phys. Rev. B* **51**, 621 (1995).
- ²⁰ G. G. Kenning, D. Chu, and R. Orbach, *Phys. Rev. Lett.* **66**, 2923 (1991); D. Chu, G. G. Kenning, and R. Orbach, *Phys. Rev. Lett.* **72**, 3270 (1994).
- ²¹ E. Vincent and J. Hammann, *J. Phys. C* **20**, 2659 (1987); F. Lefloch, J. Hammann, M. Ocio, and E. Vincent, *Physica B* **203**, 63 (1994).
- ²² T. L. Swan, R. Orbach, G. G. Wood, Y. G. Joh, J. Hammann and E. Vincent, *Bulltn. Amer. Phys. Soc.* **45**, 979 (2000).
- ²³ F. Ritort, *Phys. Rev. B* **50**, 6844 (1994); *Phil. Mag. B* **71**, 515 (1995).